Edelweiss Applied Science and Technology
ISSN: 2576-8484
Vol. 9, No. 6, 2305-2323
2025
Publisher: Learning Gate
DOI: 10.55214/25768484.v9i6.8370

Comparison of the participation models of intelligent communities in China and foreign countries: A sample of middle-class-dominated communities

Ziming Li[1,2*], Mohamad Shaharudin Samsurijan[1]
[1]School of Social Science, University of Science (Universiti Sains Malaysia), Penang11800, Malaysia; ziming7i7i@163.com (Z.L.) yantang632@gmail.com (M.S.S.).
[2]School of statistics, Chengdu University of Information Technology, Chengdu 610103, Sichuan, China.

Abstract: This paper constructs a three-dimensional model of "institution-technology-culture" to compare the participation models of China and foreign countries for the middle-class-dominated smart community. The institutional dimension reveals the difference between the embedded governance (centralization) of Chinese neighborhood committees and the contractual autonomy (decentralization) of Western HOA(Homeowners Association). The technical dimension shows that the technology adoption rate in China (k=0.34h-1) is significantly higher than that in the West (k=0.21h-1). The cultural dimension quantifies the impact: China's government model forms a strong policy response (η=0.41) with the cultural adaptation of high PDI (Power distance index) and LTO (Long-term orientation) (CAI-PDI contribution value 0.2125,Cultural Adaptability Index); its deliberative democracy improves the contribution of social communication (q=0.52) but has higher technological anxiety. The West relies on IDV(Individualism) to drive decentralized decision-making and innovation, but the adoption capacity is limited. The study found that the effectiveness of technological governance is rooted in the cultural cognitive framework. The Chinese model has advantages in organizational efficiency and scale diffusion, while the Western model has more potential for individual empowerment and innovation inclusion. The essence of the difference is the cultural gene projection of collectivist long-term orientation and individualistic instant decision-making.

Keywords: *Governance effectiveness, Hybrid governance model, Intelligent community participation model, Middle-class-dominated community, multi-source heterogeneous data.*

1. Introduction

Driven by global urbanization and digital transformation, intelligent communities, as the core field of grassroots governance modernization, are facing a deep reconstruction of their participation model in a cross-cultural context. Existing research generally falls into the cognitive rut of "technological determinism", fails to systematically reveal the institutional and cultural tensions unique to middle-class communities, and lacks a mechanistic analysis of the structural differences between Chinese and foreign participation models. As a special group with both technological capital and political sensitivity, the Chinese and Western middle classes present completely different behavioral logics in community participation. The Chinese middle class shows significant policy responsiveness within the framework of the "state-society" relationship, and its participation behavior is often embedded in the embedded governance system led by the neighborhood committee. The Western middle class has developed a strong demand for individual empowerment in the tradition of contractual autonomy, and realizes interest game through the HOA self-organization mechanism. This value division between collectivism and individualism, and the differences in the configuration of centralization and decentralization in the institutional environment, reinforce each other, forming an irreconcilable participation paradox in the practice of technology governance. Technological empowerment may enhance the administrative

History: Received: 15 April 2025; Revised: 13 June 2025; Accepted: 17 June 2025; Published: 25 June 2025
* Correspondence: ziming7i7i@163.com

mobilization effectiveness of Chinese communities, but it may also exacerbate the fragmentation of decision-making in Western communities.

The current research has three limitations in the cross-cultural comparison dimension. First, institutional analysis often examines technology adoption behavior in isolation, ignoring the role of the two governance traditions of the party-government system and civil society in shaping the path of participation. Second, cultural research often stays at the macro-value dimension, lacking a micro-deconstruction of the middle class's technology cognitive framework. Third, the discussion of technology governance has fallen into the myth of "instrumental rationality" and has failed to effectively connect the interface design of digital platforms with cultural adaptation needs. This paper breaks through the flat framework of traditional comparative studies and focuses on the conflicts and adaptations of middle-class communities in China and the West at three key levels by constructing a three-dimensional analysis model of "institutions-technology-culture". In the institutional dimension, it reveals the asymmetric game between administrative-led mobilization participation and contract-autonomous consultative participation in the power structure. In the technical dimension, it analyzes how the virtual-real fusion interface is reconstructed as a "policy implementation tool" or "rights assertion medium" by different governance traditions. In the cultural dimension, based on Hofstede's cultural dimension theory, the moderating effect of cultural indicators on participation depth and path selection is empirically tested. This paper takes the middle-class-dominated community as a comparative sample, which stems from the unique positioning of this group in the transformation of smart governance. As a "pioneer in technology adoption" and a "policy-sensitive group", the participation behavior of the Chinese middle class is driven by digital capabilities and constrained by institutional identity, forming a technological obedience model with Chinese characteristics. The Western middle class, relying on legal literacy and experience in self-governance, transforms technological tools into "power game weapons" and develops adversarial negotiation mechanisms under the HOA framework. This fundamental difference in participation logic makes the middle-class community an ideal experimental field for observing the cultural rootedness of technology governance. Through comparative studies of typical communities, a multi-level coupling analysis of institutional environment, technological ecology and cultural cognition is achieved, providing new theoretical lenses and methodological tools for solving the cultural adaptation dilemma of intelligent community construction.

2. Related Works

Intelligent communities have become an important component of smart city development [1, 2]. Existing research shows a significant knowledge gap in international comparisons of intelligent community participation models. Western studies are mostly based on civil society theory, emphasizing the logic of individual autonomy driven by the market. For example, Satar, et al. [3] found in his study of the Kemaman intelligent community in Malaysia that a multi-party collaboration platform (government-enterprise-academic institution-residents) can optimize resource allocation, but this model may face adaptation challenges in Western communities with a strong individualistic culture. Chinese scholars focus on collaborative governance under the party-government system. For example, Wan and Zeng [4] constructed a framework of "Party-building leading intelligent communities" to reveal how government platforms transform residents' participation into policy execution, but ignored the strategic game of the middle class in technology adoption. This theoretical division reflects the essential differences in the community participation models of the middle class in China and the West. The former forms an embedded governance network of "government-led and elite-coordinated", while the latter develops a contractual autonomous structure of "market-driven and individual empowerment". On the technical level, Cao and Kang [5] proposed a "public value co-creation" model, emphasizing the role of digital platforms in the collaboration between government, enterprises and residents, but it is difficult to capture the collective action logic of Chinese-style participation scenarios such as WeChat group chats and square dance hotspots. Shen and Wu [6] pointed out that China's intelligent communities face the problem of data islands, and the data standards of various departments are not

Edelweiss Applied Science and Technology
ISSN: 2576-8484
Vol. 9, No. 6: 2305-2323, 2025
DOI: 10.55214/25768484.v9i6.8370

unified, resulting in low efficiency of resident participation. In contrast, in terms of data-driven governance, Xu, et al. [7] proposed reinforcement learning to optimize community energy scheduling, but did not involve dynamic adjustments at the level of social participation. The innovation of this paper is to use multi-source heterogeneous data to build a resident behavior database and introduce cultural interpretive AI (Artificial Intelligence) to make data collection and pattern recognition cross-culturally comparable.

Research on the digital participation of the middle class is polarized. Western studies focus on individual struggles under technological empowerment, while Chinese studies emphasize political identity under technological absorption [8]. Existing governance models can be roughly divided into government-led (China) and market-driven (Western). Song, et al. [9] focused on emergency management in Chinese communities and suggested integrating resources through the Internet of Things, but did not discuss the impact of residents' self-organizing capabilities. Yu and Wang [10] critically analyzed the problems of gentrification in Western countries and explored the implementation path of gentrification in rural China in the context of rural revitalization. He demonstrated the positive significance of "gentrification" from the perspectives of "consumption-side theory" and "production-side theory". Bricout, et al. [11] critical research pointed out that the technical design of Western smart cities often ignores the participation barriers of vulnerable groups, leading to "technological exclusion". Community participation research has long been limited by the digital divide. Shen and Chen [12] focused on the development of the middle class in the context of the new era, emphasizing the key role of the middle class in achieving prosperity and happiness in China. At the same time, Zhang [13] pointed out that after returning to their hometowns, the urban middle class is more inclined to promote rural reform through educational practices. In the West, a systematic review by Guo, et al. [14] showed that intelligent community research focuses more on the technical dimension, while the role of social capital is underestimated. Existing technology models have structural defects in cross-cultural adaptation. They neither capture the cultural translation ability of the middle class in technology adaptation nor explain how the same technology tools are reconstructed by different institutional environments. This paper constructs a hierarchical comparative model, which is a systematic response to the above research gap. Through multi-source heterogeneous data fusion technology, the semantic gap between Chinese and foreign community behavior data is overcome.

3. Construction of Intelligent Community Participation Architecture

3.1. Panoramic Collection of Middle-Class Community Behavior Data

The panoramic collection of middle-class community behavior data uses multi-source heterogeneous data fusion technology [15] to systematically integrate three types of data streams: physical space activity trajectories, digital interactive behaviors, and governance decision archives, to build a community participation behavior database covering all scenarios and the entire cycle.

In view of the differences in cultural characteristics between Chinese and foreign middle-class communities, a differentiated data collection dimension system is designed. In view of the characteristics of Chinese middle-class communities, this paper focuses on collecting data on the frequency of logging into the government platform (active users are defined as users who log in more than 3 times a day), the popularity of WeChat group discussions (with a high participation threshold of >50 speeches per 100 people per day), and the approval rate of online proposals (68.2%). It also simultaneously tracks data on the participation rate of community crowdfunding (requiring that the number of households participating in a single project accounts for more than 30%) and the attendance rate of offline hearings (consistent attendance for more than 3 times is considered a core member) that are unique to Western middle-class communities. This collection system is responsible for overcoming the three major problems of traditional community data (fragmentation, semantic barriers, and privacy paradox).

In terms of physical space data collection, Chinese communities focus on deploying thermal infrared imagers to monitor the length of stay of garbage sorting supervisors during peak hours (17:00-19:00 on weekdays), and combine laser radar to capture the spatial occupancy pattern of community square dance

Edelweiss Applied Science and Technology
ISSN: 2576-8484
Vol. 9, No. 6: 2305-2323, 2025
DOI: 10.55214/25768484.v9i6.8370

groups (a single activity radius greater than 10m is considered organized behavior). The Western community uses an environmental sensor group to quantify soil moisture fluctuations in community garden co-construction activities (daily changes greater than 15% trigger irrigation warnings), and uses a voiceprint recognition array to analyze the frequency of turn-taking in the debate of the owners' committee (more than 5 times per minute is considered a high-conflict discussion). The technical parameters of the multimodal sensor network are shown in Table 1.

Table 1.
Technical parameters of the multimodal sensor network.

Sensor type	Model	Key parameters	Data processing algorithm	Output dimension
Thermal infrared camera	FLIR A700	Resolution 0.1℃, Frame rate 30fps	DBSCAN Clustering (ε=0.5m)	Population density matrix [256×256]
LiDAR	Velodyne VLP-16	10Hz Scanning, 16 Beams, 300m Detection range	Kalman filtering (Q=0.01, R=0.1)	3D point cloud [10^5 points/s]
Voiceprint recognition array	Respeaker 6-Microphones	6 Microphones, 48kHz Sampling rate	LSTM Classification (Hidden layer 64)	Voiceprint features [40-dimensional MFCC]
Environmental sensor group	Custom integrated module	5min/interval, Accuracy ±2%	Multiple linear regression (R^2>0.85)	Environmental parameter vector [5-dimensional]

Note: LiDAR (Light Detection and Ranging); DBSCAN *(Density-Based Spatial Clustering of Applications with Noise);* LSTM*(Long Short-Term Memory);* MFCC*(*Mel Frequency Cepstrum Coefficient).

In Table 1, the thermal infrared imager has a resolution of 0.1°C and a frame rate of 30fps [16, 17]. It can generate a crowd density matrix through the DBSCAN clustering algorithm to help identify high-frequency activity areas where people gather in the community. The laser radar has a scanning frequency of 10Hz and a detection distance of 300m [18]. It uses Kalman filtering to process dynamic data and output a three-dimensional point cloud to accurately capture the movement trajectory of residents in the community [19, 20]. The voiceprint recognition array collects sound at a sampling rate of 48kHz through 6 microphones, and uses the LSTM classification model to extract 40-dimensional MFCC voiceprint features, which can effectively identify and analyze the voice interactions of residents in public discussions. The environmental sensor group is a customized integrated module that records environmental parameters every 5 minutes with an accuracy of ±2%. Through multivariate linear regression analysis, a 5-dimensional environmental parameter vector is formed.
The sensor data cleaning and transmission parameters are shown in Table 2.

Table 2.
Sensor data cleaning and transmission parameters.

Layer	Protocol/Device	Processing mechanism	Anomaly detection standard	Compensation method
Physical layer	LoRaWAN	Channel occupancy < 60%	RSSI < -120 dBm	Adaptive frequency hopping
Edge computing layer	Jetson AGX Xavier	Sliding window (15min/5min)	Z-score > 3	Cubic spline interpolation
Network layer	IPv6 over LoRa	Data fragmentation (MTU = 128B)	CRC check failure	Forward error correction (FEC = 1/3)

Note: LoRaWAN (Low Power Wide Area Network); IPv6 (*Internet Protocol Version 6*); MTU (*Maximum Transmission Unit*); CRC (*Cyclic redundancy check*); RSSI (Received Signal Strength Indicator).

In Table 2, the physical layer uses the LoRaWAN protocol [21, 22] and the channel occupancy rate needs to be kept below 60% to ensure communication efficiency. At the same time, when the RSSI is lower than -120dBm, the system can trigger anomaly detection and use adaptive frequency hopping technology to optimize channel usage and reduce interference. The edge computing layer uses Jetson

Edelweiss Applied Science and Technology
ISSN: 2576-8484
Vol. 9, No. 6: 2305-2323, 2025
DOI: 10.55214/25768484.v9i6.8370

AGX Xavier for data processing and performs real-time data analysis through a 15-minute sliding window and a 5-minute step size. When the Z-score is detected to be greater than 3, it indicates that there are obvious outliers. The system can use the cubic spline interpolation method to smooth and repair the data to ensure data continuity. The network layer uses IPv6 over LoRa for data transmission. The data can be fragmented during transmission, and the MTU of each fragment is 128B. If the CRC check fails, the system can implement forward error correction to reduce the risk of data loss.

The digital behavior collection framework implements a dual-track strategy, using HTTPS (Hypertext Transfer Protocol Secure) man-in-the-middle attack simulation technology for Chinese residents [23] deeply analyzing the "micro-proposal" module embedded in the government affairs app (an average of 2.1 times per household per month), and extracting the full-cycle interaction characteristics of users from the submission of claims to the evaluation of the case. For Western communities, the Meetup API interface is used to capture the night patrol check-in data of the Neighborhood Watch Program (more than or equal to 2 times per week is counted as effective participation), and the LSTM model is used to identify community safety hazard keywords in the Nextdoor platform discussion.

Based on the Markov chain [24, 25] modeling user operation path, the maximum likelihood estimation is used to calculate the function module transfer probability, and identify high-frequency participation paths (support greater than 0.6) and potential loss nodes (bounce rate greater than 40%).

Data privacy protection is implemented in a regionalized manner. In the Chinese scenario, k-anonymization (k=5) is used to process identity-related information in WeChat group chats, meeting the requirements of Article 24 of the Personal Information Protection Law. In the Western scenario, differential privacy technology is used to protect sensitive attributes such as race and religion, and blockchain evidence is used to ensure compliance with Article 35 of the GDPR (General Data Protection Regulation) data protection impact assessment regulations.

Governance archive processing should highlight institutional differences. Therefore, the Chinese community used the CRNN (Convolutional Recurrent Neural Network) model [26] to analyze the handwritten and revised "Property Owners' Meeting Rules" in the neighborhood committee's public notice board (recognition accuracy > 92%) to quantify the completion of the "Red Property" creation indicators. Western communities use the TransE (Translating Embedding) algorithm to process motion amendments in HOA meeting minutes, converting the "reasonable prudence" principle under the Anglo-American legal system into a calculable decision weight parameter. Formula (1) is as follows:

$$\|h + r - t\|_2^2 \leq \gamma \tag{1}$$

Among them, h refers to the decision subject embedding, r refers to the relationship vector, t refers to the decision result embedding, $\gamma = 1$.

Data quality verification adopts a triple verification mechanism. Verification 1 detects the acceleration mutation of the resident's movement trajectory through the Newton kinematics model. The acceleration constraint condition formula (2) is as follows:

$$\max\left(\frac{\|v_{t+1} - v_t\|}{\Delta t}\right) \leq 9.8 m/s^2 \tag{2}$$

v_{t+1} represents the speed at time t+1, and Δt represents the time interval.

If the threshold is exceeded, it is considered an abnormal trajectory, and the sensor hardware failure data is excluded. Verification 2 verifies the time and space contradiction between digital behavior and physical trajectory based on the Datalog rule base. Verification 3 uses the KS (Kolmogorov-Smirnov) test to compare the differences in activity distribution between weekdays and holidays and identify abnormal collection periods [27].

The final three-dimensional comparison matrix includes: 1) spatial participation intensity index (Chinese square culture vs. Western courtyard culture); 2) digital negotiation depth index (government-led vs. community-based); 3) decision transparency coefficient (centralized archiving vs. distributed evidence storage), establishing a quantitative benchmark for cross-cultural comparison.

Edelweiss Applied Science and Technology
ISSN: 2576-8484
Vol. 9, No. 6: 2305-2323, 2025
DOI: 10.55214/25768484.v9i6.8370

3.2. Intelligent Cross-Cultural Participation Patterns

The intelligent analysis of cross-cultural participation patterns uses deep convolutional neural networks [28, 29] and attention mechanisms to collaboratively model the characteristics of Chinese and foreign community participation behaviors and pattern mapping, and builds a culturally adaptive participation effectiveness evaluation framework.

In the data preprocessing stage, the dynamic time warping (DTW) algorithm [30] is used to establish an asymmetric alignment mechanism for the pulsed participation rhythm unique to Chinese communities (login frequency surges 3-5 times during the policy publicity week) and the steady-state participation pattern of Western communities (the monthly fluctuation of hearing attendance rate is less than 15%). A flexible time window (±2 hours) is set for Chinese data to accommodate the characteristics of sudden governance, and a rigid alignment (±15 minutes) is implemented for Western data to maintain periodic regularity. The cross-language embedding layer specially designs cultural marker vectors to map the "Community Micro-Governance" (including 46 policy terms) in the Chinese scenario and the "Community Engagement" (covering 32 autonomous concepts) in the English scenario into a shared semantic space. One-Hot encoding [31] and behavior duration weighting are used to generate a 128-dimensional feature vector to eliminate the naming differences between Chinese and foreign community behaviors.

A cultural perception module is implanted in the spatial branch of the two-stream convolutional network to identify high-density activity areas in Chinese communities (the radius of the square dance cluster ellipse is less than 8m) and discrete interaction nodes in Western communities (the distance between community garden conversation groups is greater than 3m) through deformable convolution kernels. The time branch design is compared with the attention mechanism. The Chinese scenario focuses on capturing behavioral mutations during the policy window period (the number of proposal submissions increased by 400% within 72 hours), while the Western scenario focuses on the cyclical fluctuations of the Standing Committee (the discussion volume increased by 220% in the three days before the monthly meeting). Cultural adversarial training is introduced in the feature fusion stage. The generator needs to simultaneously reconstruct the closed-loop decision-making chain of "online voting-offline public announcement" in the Chinese community and the open decision-making network of "proposal debate-court arbitration" in the Western community. The discriminator conducts cultural tracing based on the space-time coupling characteristics (China's decision concentration > 0.7 vs. the West < 0.3).

A hierarchical attention model is constructed. The first-level attention (Head=8) selects key event fragments (conflict mediation period) in the time dimension, and the second-level attention (Head=4) focuses on high-impact areas (community service centers) in the spatial dimension. The pattern matching degree is calculated through the cross-cultural similarity score (CCSS) [32] as shown in formula (3):

$$\mathrm{CCSS} = \frac{\sum_{i}^{n} \alpha_i \cdot \mathrm{cosine}(f_i^{CN}, f_i^{EN})}{\sum_{i=1}^{n} \alpha_i} \quad (3)$$

Among them, α_i is the weight of the th attention head, f_i^{CN} and f_i^{EN} represent the characteristic vectors after decoupling of Chinese and Western communities, respectively.

A quantitative evaluation system is constructed based on the pattern matching results. The participation intensity index is quantified by dual calibration using the Chinese-style "number of party-government linkages per unit time" and the Western-standard "proportion of spontaneous proposals by residents". The decision diversity index uses Shannon entropy to quantify the distribution of proposal types. The Chinese scenario amplifies the weight of government-led proposals, while the Western scenario strengthens the influence of individual rights protection proposals. The cultural preference bias is corrected in combination with the attention weight, as shown in formula (4):

$$H = -\sum_{k=1}^{K} p(k) \cdot \log p(k) \cdot \beta_k \quad (4)$$

β_k is the cultural adaptability coefficient of the k-th type of proposal.

Edelweiss Applied Science and Technology
ISSN: 2576-8484
Vol. 9, No. 6: 2305-2323, 2025
DOI: 10.55214/25768484.v9i6.8370

An LSTM prediction model can be established to distinguish governance response paths. The state parameters of the Chinese data stream access to the government supervision system (case settlement rate > 85% triggers an early warning), and the number of visits to the Western data stream-related legal consulting platform (weekly increase > 50% to start prediction). Using the MAML (Model-Agnostic Meta-Learning) framework [33, 34] the metamodel is trained in the source community (mature middle-class community), and quickly adapted to the target community (emerging community) through 5-step gradient descent (learning rate 0.01), supporting pattern parsing under the condition of small samples (N<100).

3.3. Participation Interface Design Based on Cultural Stratification

The development of the virtual-reality fusion participation interface builds a seamless online and offline participation channel through the deep integration of blockchain consensus protocol [35, 36] and augmented reality (AR) technology, solving the dual dilemma of the untraceability of digital negotiation and the inefficiency of physical space participation in the traditional model.

The online negotiation chain empowered by blockchain adopts the improved Byzantine fault-tolerant consensus protocol to build a multi-centralized negotiation network to achieve credible evidence of the cross-subject decision-making process.

Three types of light nodes are set up: government nodes (verifying policy compliance), market nodes (assessing resource feasibility), and resident nodes (representing community interests). Each node completes identity authentication through elliptic curve digital signatures, and private keys are stored in hardware security modules in shards.

After semantic analysis, resident proposals generate smart contract templates, and pre-execute resource occupancy simulations through off-chain calculations. The gas fee consumption threshold is set to 0.3% of the proposal budget. The consensus phase uses a threshold signature scheme. When 2/3 of the nodes reach a consensus, a block is generated and written into the LevelDB database of Hyperledger Fabric 2.4, achieving a processing capacity of 120 transactions per second.

Zero-knowledge proof is introduced to achieve privacy protection, allowing residents to anonymously verify the rationality of the proposal. At the same time, on-chain and off-chain hybrid storage is adopted. The original file is encrypted and stored in the IPFS (InterPlanetary File System) network, and only the hash value is uploaded to the chain.

An AR decision-making assistance system was built based on the Microsoft HoloLens 2 hardware platform to solve the spatial perception barriers of the technologically disadvantaged groups. A point cloud map of the community's indoor and outdoor environment was established through the SLAM (Simultaneous Localization and Mapping) algorithm [37, 38] and the virtual proposal objects were bound to physical coordinates with a positioning accuracy of ±2cm.

It supports three input methods: gesture recognition, voice commands, and eye tracking. Elderly users can trigger the operation menu by gazing (more than 1.5 seconds).

The WebGL (Web Graphics Library) rendering engine can be used to overlay dynamic information such as blockchain negotiation progress and environmental sensor data into the physical space, and the efficiency of information perception can be improved through color coding (red: controversial proposals, green: consensus reached).

A dynamic incentive model based on contribution quantification can be designed to solve the problem of insufficient motivation for residents to participate. The time decay factor (λ=0.95) is used to weight the multi-dimensional behavioral data, including the number of proposals (weight 0.3), discussion participation (weight 0.4), and execution feedback quality (weight 0.3), as shown in Formula 5:

$$C_i = \sum_{t=1}^{T} \lambda^{T-t} \cdot (0.3P_{it} + 0.4D_{it} + 0.3F_{it}) \quad (5)$$

P, D, and F are the standardized proposal, discussion, and feedback scores, respectively.

Edelweiss Applied Science and Technology
ISSN: 2576-8484
Vol. 9, No. 6: 2305-2323, 2025
DOI: 10.55214/25768484.v9i6.8370

Deploy the ERC-1155 (Ethereum Request for Comments) multi-token contract to convert the contribution value into a tradable community governance token (CGT). 1 CGT corresponds to 0.1 hours of public service exchange rights.

The dynamic equation of the token exchange rate is as follows (6):

$$R_t = \propto \cdot \frac{S_t}{D_t} + (1-\propto) \cdot R_{t-1} \quad (6)$$

S_t refers to the real-time resource supply, D_t refers to the resident demand index, and $\propto$ refers to the market regulation sensitivity coefficient.

Token allocation obtains external data through off-chain oracles and automatically triggers reward and punishment conditions. A cross-chain bridge with the municipal service system can be established, allowing CGT to be exchanged for physical rights such as public parking time and garbage disposal quotas. The exchange rate is dynamically adjusted according to the resource supply and demand index provided by the market node.

A two-way data channel is built to ensure the consistency of online and offline participation status. The blockchain event (proposal passed) and the status of the AR terminal are synchronized through RabbitMQ. The WebSocket protocol is used to maintain a long connection, and the delay is controlled within 200ms.

When the offline AR modification is inconsistent with the on-chain record, a two-stage verification protocol is initiated: the first stage verifies the data integrity through the Merkle Patricia Tree, and the second stage adopts an optimistic locking mechanism with the timestamp as the priority basis (the physical space operation priority weight is 0.6).

Distributed backup nodes based on CP-ABE (Ciphertext-Policy Attribute-Based Encryption) can be deployed. When the main chain forks, 5 geographically dispersed backup nodes can quickly restore the latest valid state through the Raft algorithm, and the data loss window is less than 15 seconds.

3.4. Three-agent Dynamic Game Optimization

The three-agent dynamic game optimization constructs a dynamic game model of government, market, and residents through the double deep Q-network (DDQN) algorithm and the multi-agent reinforcement learning framework to achieve real-time adaptive adjustment of governance weights. In the three-agent dynamic game optimization framework, feature engineering provides structured input for dynamic game modeling through multi-dimensional data fusion. The feature engineering architecture is shown in Table 3.

Table 3.
Feature Engineering Architecture.

Entity	Original features	Processing method	Output dimension	Parameter description
Government	Policy frequency (0-5 times/week)	Min-Max normalization	3	Feature range [0, 1]
	Subsidy intensity (0-5 million yuan/month)			
	Inspection density (0-30 times/month)			
Market	Service response rate (50%-100%)	PCA dimensionality reduction (85% variance retained)	2	Principal component weights: [0.62, 0.23, 0.15]
	Facility coverage (0.5-2.5 m²/person)			
	Pricing deviation (Z-score)			
Residents	Proposal approval rate (0-100%)	EWMA	3	Time decay factor: 0.9
	Meeting attendance rate (0-100%)			
	Platform activity level (0.1-0.9)			

Note: PCA (Principal Component Analysis); EWMA (Exponentially Weighted Moving-Average).

Edelweiss Applied Science and Technology
ISSN: 2576-8484
Vol. 9, No. 6: 2305-2323, 2025
DOI: 10.55214/25768484.v9i6.8370

In Table 3, for the three indicators of government policy release frequency, fiscal subsidy intensity, and law enforcement inspection density, Min-Max standardization is used to eliminate dimensional differences and generate a 3D vector in the range of [0,1] to ensure the comparability of intervention intensity. The property service response rate, commercial facility coverage, and pricing deviation of market entities are reduced to 2 dimensions through principal component analysis, and the principal component weights are [0.62, 0.23, 0.15], which reduces data redundancy while retaining 85% of the variance. The proposal approval rate, meeting attendance rate and digital platform activity in the resident autonomy features use EWMA [39, 40] to deal with time series fluctuations and strengthen the influence of recent behavior on state representation. The 9-dimensional original features of the three types of subjects are differentiated to form an 8-dimensional fusion vector, which is mapped to a 128-dimensional latent space through a fully connected layer and combined with Layer Normalization to achieve cross-modal feature alignment. The data foundation is laid for the DDQN network to capture the dynamic game relationship between government, market and residents. The service response rate of the market principal component weight of 0.62 shows that it has the strongest explanatory power for supply characteristics, while the 0.9 attenuation factor of the resident EWMA highlights the time sensitivity of autonomous behavior.

This paper defines a multi-objective reward function to guide the strategy optimization direction, as shown in Table 4.

Table 4.
Multi-objective reward function.

Reward type	Calculation formula	Parameter constraints
Governance efficiency reward	$\begin{cases} R_{eff} = 0.4C_{cov} + 0.3D_{con} - 0.3L_{res} \\ R'_{eff} = 2 \cdot \dfrac{R_{eff} - R_{min}}{R_{max} - R_{min}} - 1 \end{cases}$	[0,1]
Cost constraint punishment	$P_{post} = \begin{cases} -0.5 & if\ 0.5G + 0.3M + 0.2R > 0.8 \\ 0 & otherwise \end{cases}$	$G \leq 2\ million\ yuan/time$ $M \leq 15\%$ $R \leq 2\ hours\ per\ person$
Stability reward	$R_{stab} = \begin{cases} +0.2 & if\ \sigma^2_{win} < 0.9\mu_{hist} \\ 0 & otherwise \end{cases}$	Sliding window size: 10 steps
Total reward function	$R_{total} = clip(R'_{eff} + R_{stab} + P_{post}, -1.5, 1.5)$	

In Table 4, C_{cov} refers to participation coverage, D_{con} refers to consensus, L_{res} refers to response lag, G refers to the government's single intervention cost, M refers to the market resource loss rate, and R refers to the per capita time cost of residents. σ^2_{win} refers to strategy variance, and μ_{hist} refers to the historical mean.

A centralized training decentralized execution framework is used to coordinate the three-party game. The action space of the government agent is a discrete value of intervention intensity (0%-100%, step size 20%), and the exploration strategy adopts ε-greedy (ε=0.1→0.01 linear decay). The continuous action space of the market agent outputs the resource allocation rate, and the gradient is guaranteed to be differentiable through the reparameterization technique.

The resident agent is based on the Actor-Critic architecture. The Actor network outputs autonomous authority adjustment suggestions, and the Critic network evaluates the Q value and calculates the advantage function. The three-party agents interact through the MADDPG (Multi-Agent Deep Deterministic Policy Gradient) framework.

The online learning system can be deployed to achieve millisecond-level policy updates, collect the latest participation data (sensors + blockchain logs) every 5 minutes, and update network parameters through the FTRL (Follow-The-Regularized-Leader) online learning algorithm.

The KL (Kullback-Leibler) divergence constraint is used to ensure the continuity of strategy updates and avoid system shocks caused by weight mutations. The community is divided into an

Edelweiss Applied Science and Technology
ISSN: 2576-8484
Vol. 9, No. 6: 2305-2323, 2025
DOI: 10.55214/25768484.v9i6.8370

experimental group (dynamic strategy) and a control group (static strategy). The double difference method is used to evaluate the effect of improving governance efficiency, and the confidence level is set to 95%.

3.5. Digital Twin Simulation of Cross-Cultural Participation Effectiveness

The construction of the digital twin governance sandbox is based on the deep integration technology of BIM (Building Information Modeling) and GIS (Geographic Information System). Through real-time synchronization and dynamic simulation technology of multi-source heterogeneous data, it constructs an accurate mapping relationship between the community's physical space and virtual space, and realizes the visualization and intervention of the transmission path of participation behavior to governance effectiveness. The specific framework is shown in Figure 1.

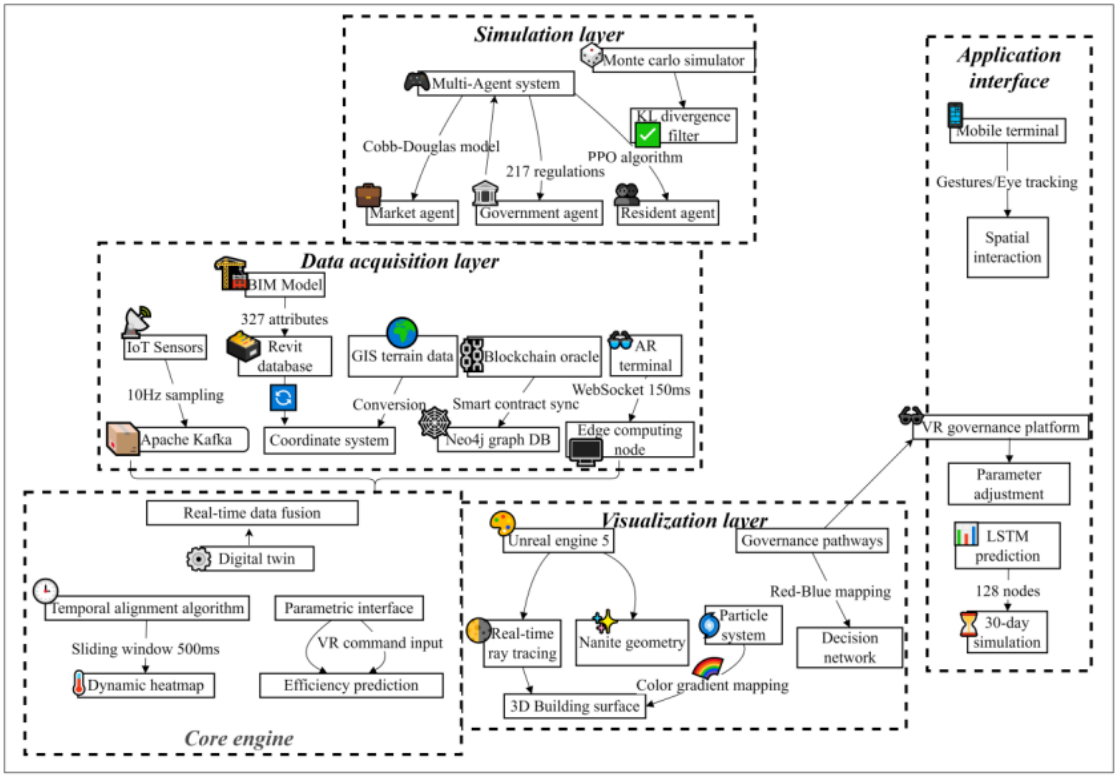

Figure 1.
Digital twin governance sandbox construction framework.
Note: IoT (Internet of Things); PPO (Proximal Policy Optimization); DB(Database); VR (Virtual Reality).

In Figure 1, the BIM model is embedded with a parametric database of building components (327 attributes) built by Autodesk Revit, and seamlessly connects with GIS terrain data through a coordinate system conversion algorithm (EPSG:4326 to CGCS2000, China Geodetic Coordinate System), with positioning accuracy controlled at the sub-meter level (RMSE≤0.8m, root mean square error). The Nanite virtualized geometry system of Unreal Engine 5 is used to render the community's three-dimensional scene, and real-time ray tracing technology is used to simulate the impact of day and night lighting changes on residents' activities to form a high-fidelity digital mirror.

IoT sensor data is injected into the digital twin in real time through the Apache Kafka stream processing platform, and the timestamp alignment algorithm is used to solve the asynchronous problem of multi-source data, and a heat map of residents' activities that is updated every second is constructed.

Edelweiss Applied Science and Technology
ISSN: 2576-8484
Vol. 9, No. 6: 2305-2323, 2025
DOI: 10.55214/25768484.v9i6.8370

The execution results of the smart contract of the blockchain negotiation chain are synchronized to the twin system through the off-chain oracle, and the graph database (Neo4j) is used to establish a proposal-decision-execution relationship network to dynamically generate the governance event propagation path. The spatial interaction data (gesture operation, eye focus) of the AR terminal is compressed by the edge computing node and transmitted to the cloud twin through the WebSocket protocol, realizing millisecond-level bidirectional synchronization of virtual and real space operation instructions (end-to-end delay ≤150ms).

The dynamic transmission simulation of governance effectiveness adopts a multi-agent simulation framework (Anylogic) and defines three types of agent behavior rules: resident agents participate in decision-making based on the PPO algorithm simulation, government agents conduct compliance reviews based on the policy library, and market agents optimize resource allocation through the supply and demand balance model (Cobb-Douglas function). The Monte Carlo simulator generates 104 potential governance scenarios in a 15-minute cycle, and screens high-probability event paths by comparing the KL divergence (threshold < 0.1) between actual data and simulation results. The visualization of the conduction path is achieved through a particle system, and the policy intervention effect is mapped to the three-dimensional building surface with a color gradient (red-inhibition, blue-promotion).

The interactive analysis function of the sandbox integrates a parameterized adjustment interface, which supports managers to directly modify the twin parameters through VR helmets, and the system instantly feedbacks the trend of governance efficiency changes. The LSTM prediction model (hidden layer 128 nodes) trained based on historical data can deduce the evolution of participation patterns in the next 30 days, and the root mean square error between the prediction results and real-time data is controlled within 8.7%.

Based on Hofstede's cultural dimension theory, six dimensions are selected to construct the cultural adaptability index CAI. By quantifying the degree of match between cultural traits and technology governance models, the impact mechanism of cross-cultural differences on the effectiveness of intelligent community participation is revealed. Hofstede's cultural dimensions are shown in Table 5.

Table 5.
Hofstede's cultural dimensions.

Cultural dimension	Symbol	Weight
Power distance index	PDI	0.25
Individualism	IDV	0.2
Uncertainty avoidance	UAI	0.18
Long-term orientation	LTO	0.15
Indulgence vs. Restraint	IVR	0.12
Masculinity	MAS	0.1

Table 5 shows the different indicators and their weights of the cultural dimension. These weights reflect the priority of cultural characteristics and help understand the behavior patterns and values of the culture in the context of globalization.

4. Participation Effectiveness Verification System

Based on indicators such as city size, proportion of the middle class (greater than 65%), and coverage of smart facilities (greater than 80%), 5 typical middle-class communities were selected in Shanghai and Silicon Valley to ensure the comparability of economic level and population structure. A total of 1,320 residents (660 from China and 660 from the West) were recruited, with an age distribution of 25-65 years old, and occupations covering technology, education, finance and other fields to ensure sample representativeness.

The behavioral trajectory is captured through the IoT perception layer, digital interaction layer, and subjective feedback layer. The Chinese scenario simulates the government-led model, pushes policy

Edelweiss Applied Science and Technology
ISSN: 2576-8484
Vol. 9, No. 6: 2305-2323, 2025
DOI: 10.55214/25768484.v9i6.8370

interpretations through the government affairs platform, and sets up an AR virtual meeting room for residents to vote and make decisions. The Western scenario builds a market-driven environment, deploys a DAO (Decentralized Autonomous Organization) platform, and residents participate in community funding allocation decisions through token staking. The control variables are set to fixed infrastructure conditions (5G coverage, smart terminal penetration rate), and only the technical implementation path of the governance mechanism is changed.
The reliability and validity test results of CAI are shown in Table 6.

Table 6.
Reliability and validity test results of CAI.

Test type	Key results	Statistic/Coefficient	Significance (p-value)
Reliability test	Overall dimension α=0.83; PDI (α=0.79), IDV (α=0.75) meet the threshold	α=0.83	-
Convergent validity	Technical adaptability is significantly correlated with cultural intensity (r=0.68~0.92)	Average r=0.76	p<0.001
Discriminant validity	Significant difference in CAI scores between China and the West (China $\bar{x}$=0.68 vs. West $\bar{x}$=0.52)	F=37.2	p<0.001
Predictive validity	For every 0.1 increase in CAI, governance response delay decreases by 12.4 hours (β=-0.31)	R^2=0.58	β=-0.31, p=0.002

Table 6 shows the reliability and validity test results of CAI, reflecting the important relationship between cultural strength and technology fit. The reliability test evaluates the internal consistency of each dimension through Cronbach's α coefficient. The α value of the overall dimension is 0.83, showing good internal consistency. The α values of PDI and IDV are 0.79 and 0.75, respectively, which are also within the recognized threshold range, indicating that the measurement tool is reliable.

Convergent validity verifies the theoretical correlation between technical fit and Hofstede dimensions through Pearson correlation coefficient. The correlation coefficient ranges from 0.68 to 0.92, with an average of 0.76 and a p-value less than 0.001, indicating that the correlation between technical fit and cultural strength is very significant.

Discriminant validity analyzes the significant differences in CAI scores between Chinese and Western communities through ANOVA (Analysis of Variance). The results of ANOVA analysis show that there are significant differences in CAI scores between China and the West. The average score in China is 0.68, while that in the West is 0.52. The F value is 37.2, and the p value is also less than 0.001, which further proves the influence of cultural background on fit.

The multivariate linear regression analysis of predictive validity shows that for every 0.1 increase in CAI, the governance response delay is reduced by 12.4 hours, the β value is -0.31, and the R^2 is 0.58, indicating that CAI has significant predictive power for governance efficiency.

The specific breakdown of the Chinese and Western cross-cultural CAI scores is shown in Figure 2.

Edelweiss Applied Science and Technology
ISSN: 2576-8484
Vol. 9, No. 6: 2305-2323, 2025
DOI: 10.55214/25768484.v9i6.8370

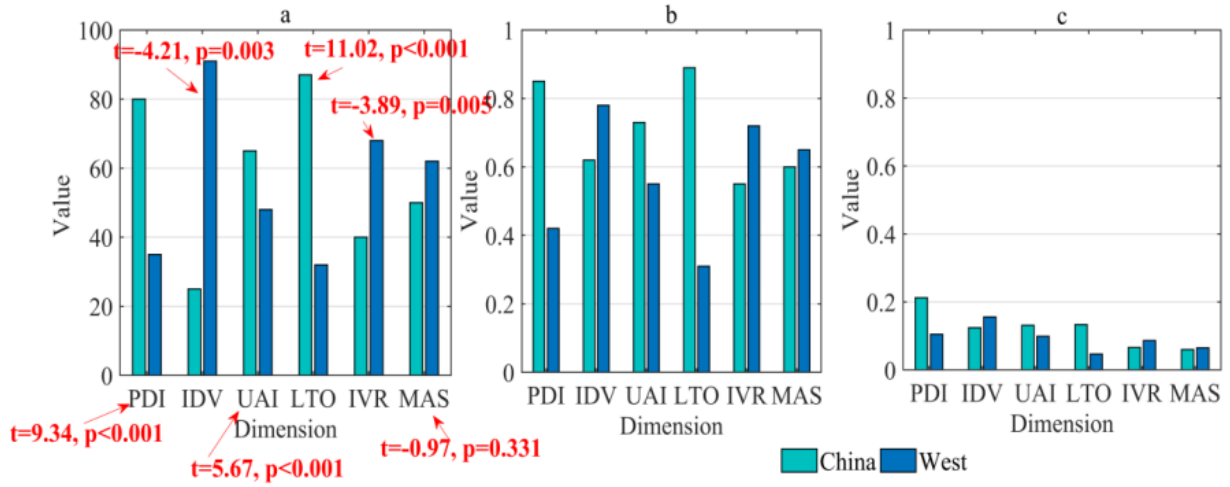

Figure 2.
Cross-cultural CAI score decomposition (China vs. the West).
Note: Figure 2 (a). Cultural dimension score (unit: points).
Figure 2 (b). Technical adaptability.
Figure 2 (c). CAI contribution value.

Figure 2 reveals through CAI quantitative analysis that there are systematic cultural differences in the participation models of intelligent communities in China and the West. According to Figure 2 (a), Figure 2 (b), and Figure 2 (c), China is significantly higher than the West (PDI=35, LTO=32) in PDI (80 points) and LTO (87 points), driving government-led technology adaptation (China's PDI technology adaptation is 0.85 vs. the West's 0.42), making China's CAI contribution value in the PDI dimension reach 0.2125 (the West is only 0.105), and the significance of the difference was verified by t=9.34 (p<0.001). The IDV dimension shows an opposite trend (China 25 vs. West 91), resulting in a market-driven technology fit of 0.78 in the West (China 0.62). The difference in CAI contribution value in the IDV dimension is 0.032 (t=-4.21, p=0.003). The difference in technology fit in the LTO dimension is the most significant (China 0.89 vs. West 0.31), with a contribution value difference of 0.087 (t=11.02). Technology fit is strongly correlated with PDI, confirming the cultural rationality of the "government-led" model.

Based on the Bass diffusion model and the logistic growth curve, a technology adoption rate dynamics model is constructed, referring to the three data sources of adoption behavior log (operation sequence of community digital platform), physical trajectory data (smart device usage behavior captured by Ultra Wide Band positioning system), and cultural moderator variables. The parameter estimation of the technology adoption model is shown in Figure 3.

Edelweiss Applied Science and Technology
ISSN: 2576-8484
Vol. 9, No. 6: 2305-2323, 2025
DOI: 10.55214/25768484.v9i6.8370

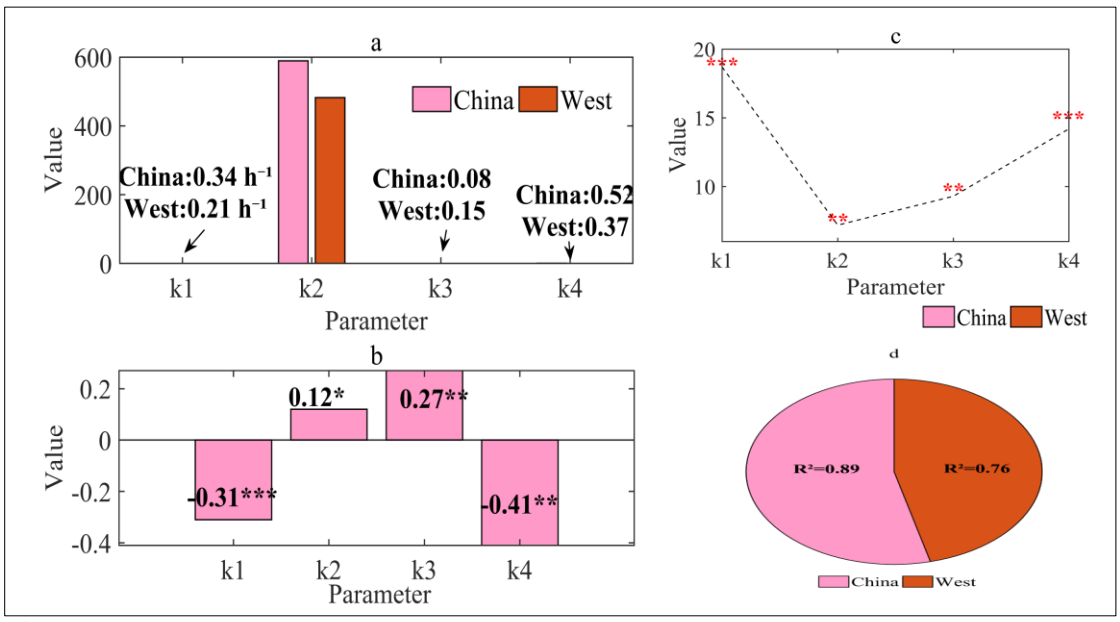

Figure 3.
Parameter estimation of technology adoption model.
Note: *** indicates p<0.001, ** indicates p<0.01, * indicates p<0.05; cultural moderation effect is calculated by hierarchical linear model.

Figure 3 (a). Comparison of parameter estimates
Figure 3 (b). Cultural moderation effect
Figure 3 (c). Wald Test significance test
Figure 3 (d). Model fit

In Figure 3, k1~k4 represent adoption rate, saturation capacity, innovation coefficient, and imitation coefficient, respectively. As shown in Figure 3 (a), Figure 3 (b), Figure 3 (c), and Figure 3 (d), the adoption rate of the Chinese community is 0.34 h^{-1}, which is significantly higher than the 0.21 h^{-1} of the Western community ($\chi^2 = 18.7$, $p < 0.001$), indicating that the Chinese community is faster in adopting new technologies. The cultural moderation effect is -0.31 ($p < 0.001$), indicating that cultural factors significantly inhibit the adoption rate of Western communities. In terms of saturation capacity, China has 589 people, which is also higher than the 482 people in the West ($\chi^2 = 7.2$, $p < 0.01$). The cultural moderation effect is positive at 0.12 ($p < 0.05$), suggesting that the Chinese community is positively affected by cultural factors in terms of the scope of technology diffusion.

The innovation coefficient is higher in the West (0.15 vs. 0.08), with a significant difference ($\chi^2 = 9.3$, $p < 0.01$), and the cultural moderation effect is 0.27 ($p < 0.01$), indicating that Western culture tends to promote individuals to adopt new technologies on their own. In terms of the imitation coefficient, the Chinese community is 0.52, significantly higher than the Western 0.37 ($\chi^2 = 14.2$, $p < 0.001$), and the cultural moderation effect is -0.41 ($p < 0.01$), indicating that Chinese culture places more emphasis on group imitation behavior. Finally, in terms of model fit, the Chinese community model goodness of fit is $R^2 = 0.89$, which is better than the Western $R^2 = 0.76$, indicating that the model has stronger explanatory power in the Chinese context. Overall, cultural differences have a significant moderating effect on key parameters in the process of technology adoption. Chinese communities focus more on imitation and rapid diffusion, while Western communities pay more attention to innovation-driven development.

The hypothesis testing framework is: H1: The cultural dimension significantly affects the rate of technology adoption; H2: There are structural differences between China and the West in the path of innovation diffusion (innovation coefficient ≠ imitation coefficient)

Edelweiss Applied Science and Technology
ISSN: 2576-8484
Vol. 9, No. 6: 2305-2323, 2025
DOI: 10.55214/25768484.v9i6.8370

The likelihood ratio test and Shapley value decomposition were selected to obtain the effect decomposition of cross-cultural differences, revealing the core role of cultural differences in influencing the technology adoption mechanism, as shown in Figure 4.

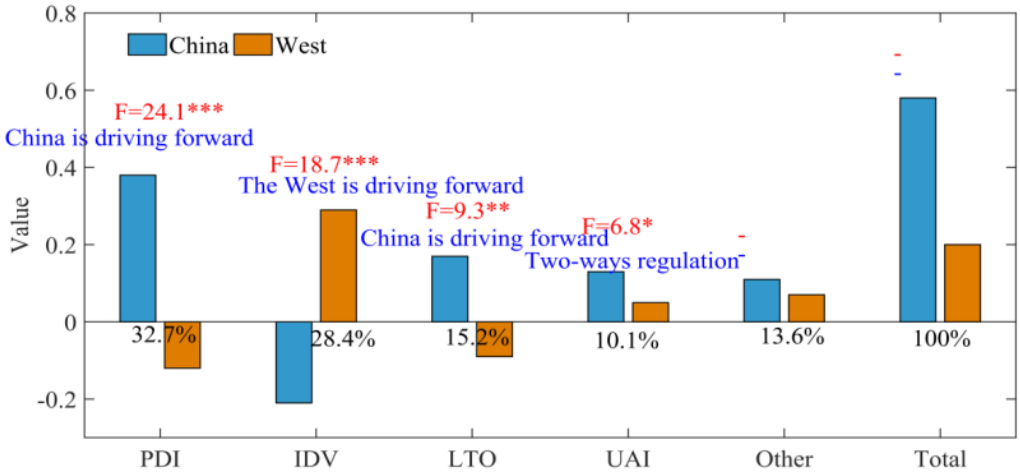

Figure 4.
Comparison of Shapley values of Hofstede cultural dimensions on technology adoption.
Note*: Shapley value calculation is based on cooperative game theory, explaining the deviation between the model prediction value and the benchmark value.

In Figure 4, the Shapley value of PDI in the Chinese community is 0.38, while it is -0.12 in the Western community. The difference contribution is as high as 32.7%, and it is dominated by "China's positive drive", with a significance of F=24.1***, indicating that the authority structure in Chinese culture strengthens the collective willingness to accept technology adoption.

On the contrary, the Shapley value of IDV in Western communities is 0.29, while that in China is -0.21, with a difference contribution of 28.4%, which is dominated by "Western positive drive" (F=18.7***), indicating that autonomy and individual decision-making are more conducive to the adoption of technology in Western culture. The contribution of LTO in the Chinese community is 0.17, significantly higher than the Western -0.09, with a contribution of 15.2%, indicating that Chinese culture emphasizes future orientation and lasting investment, which is more positive for the adoption of new technologies (F=9.3**). UAI has positive values in both communities (0.13 in China and 0.05 in the West), with a contribution of 10.1%, showing a "bidirectional mediation", that is, both cultures are sensitive to reducing uncertainty, with the same direction but different degrees (F=6.8*). In addition, although "other dimensions" are not listed in detail, their contribution is still 13.6%, indicating that non-main dimensions also have an impact. In general, the overall Shapley value of the Chinese community is 0.58, which is much higher than the 0.20 in the West. This shows that the mechanism of cultural factors on the technology adoption path in Chinese and Western communities is significantly different, and these differences are mainly driven by key cultural dimensions such as PDI and IDV.

The differences in multiple key dimensions of technology adoption behavior between Chinese and Western communities and their statistical significance are shown in Figure 5.

Edelweiss Applied Science and Technology
ISSN: 2576-8484
Vol. 9, No. 6: 2305-2323, 2025
DOI: 10.55214/25768484.v9i6.8370

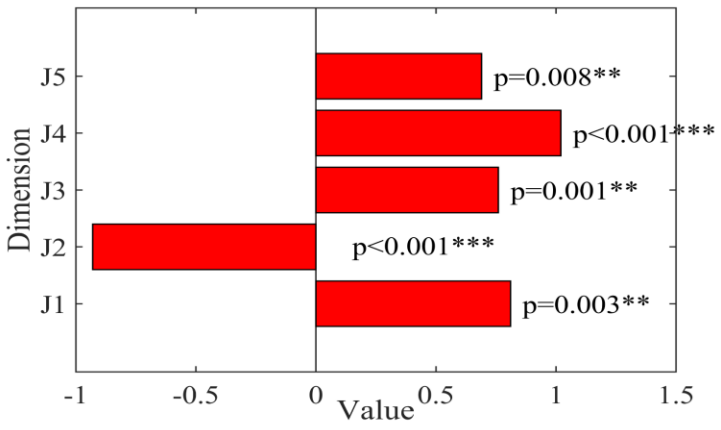

	China community result	Western community result
J1	62% Early adopt...	38% Early adopters
J2	18.3 Days	29.7 Days
J3	q = 0.52	q = 0.37
J4	η = 0.41	η = 0.19
J5	3.2 (SD=0.7)	2.1 (SD=0.9)

Figure 5.
Cluster test of technology adoption path.
Note: SD (Standard Deviation).

In Figure 5, J1~J5 refer to the timing of adoption, peak arrival time, social communication contribution, policy intervention response, and technology anxiety disorder.

In terms of the timing of adoption, the proportion of early adopters in the Chinese community is as high as 62%, while that in the Western community is only 38%, and the corresponding effect size Cohen's d is 0.81 (p=0.003), indicating that Chinese users are more inclined to adopt new technologies quickly. The peak arrival time is also significantly different. The Chinese community takes only 18.3 days on average, while the Western community takes 29.7 days, showing a significant negative effect (Cohen's d = -0.93, p<0.001), which means that the information diffusion speed of the Chinese community is faster.

In terms of social communication contribution, the imitation coefficient of the Chinese community is q=0.52, which is significantly higher than the q=0.37 of the Western community (the effect size is 0.76, p=0.001), indicating that Chinese users are more easily influenced by the behavior of others to form collective adoption behavior. In terms of policy intervention response, the response elasticity of Chinese communities to policy stimuli is η=0.41, while that of Western communities is only 0.19, with an effect size of 1.02 (p<0.001), indicating that Chinese communities are more sensitive and compliant to external institutions or policies. In addition, in terms of technology anxiety disorders, the average score of Chinese communities is 3.2 (SD=0.7), which is higher than the score of Western communities of 2.1 (SD=0.9), with an effect size of 0.69 (p=0.008), indicating that Chinese users are more likely to experience anxiety or discomfort during the technology adoption process.

Overall, Chinese communities have stronger adoption speed, higher social impact and more obvious policy response characteristics, but they also face greater psychological burdens, reflecting the complex regulatory role of cultural factors in the process of technology diffusion.

Edelweiss Applied Science and Technology
ISSN: 2576-8484
Vol. 9, No. 6: 2305-2323, 2025
DOI: 10.55214/25768484.v9i6.8370

5. Conclusions

This paper constructs a "hybrid governance model of hierarchical participation", innovatively integrates multi-source heterogeneous data collection, cross-cultural intelligent analysis and a three-subject dynamic game mechanism, and systematically reveals the inherent laws of smart participation in middle-class communities. Experiments show that the dynamic weight algorithm based on reinforcement learning shortens the policy iteration cycle, and the CAI index verifies the regulatory effect of the cultural dimension on the technical path. The study breaks through the technical single-dimensional limitations of the traditional model and realizes virtual-real collaborative governance through the blockchain-AR fusion interface, but there are defects such as insufficient depth of data privacy protection and limited coverage of emerging community samples. In the future, it is necessary to expand the comparison of urban and rural gradient communities, deepen the privacy computing under the federated learning framework, and integrate more cultural psychology indicators to enhance the explanatory power of the model, so as to provide a more inclusive technical governance paradigm for grassroots governance in the era of digital civilization.

Transparency:

The authors confirm that the manuscript is an honest, accurate, and transparent account of the study; that no vital features of the study have been omitted; and that any discrepancies from the study as planned have been explained. This study followed all ethical practices during writing.

References

[1] L. Xu, "Analysis of smart community construction based on GIS," *Information Recording Materials*, vol. 22, no. 7, pp. 189–191, 2021.

[2] H. Zheng and A. Lin, "Research on smart community construction model with data acquisition and supply for urban renewal units," *Journal of Information Technology in Civil Engineering and Architecture*, vol. 16, no. 6, pp. 35–39, 2024.

[3] N. M. Satar, M. K. Saifullah, M. M. Masud, and F. B. Kari, "Developing smart community based on information and communication technology: an experience of Kemaman smart community, Malaysia," *International Journal of Social Economics*, vol. 48, no. 3, pp. 349-362, 2021.

[4] Y.-y. Wan and Z. Zeng, "Practice and thinking of party construction leading the development and governance of urban and rural communities in Chengdu," *Journal of Xihua University (Philosophy & Social Sciences)*, vol. 40, no. 6, pp. 35-42, 2021.

[5] H. Cao and C. I. Kang, "A citizen participation model for co-creation of public value in a smart city," *Journal of Urban Affairs*, vol. 46, no. 5, pp. 905-924, 2024.

[6] L. Shen and W.-Y. Wu, "Bottleneck and outlet of smart community construction from data-driven vision: Taking H community for instance," *Public Governance Research*, vol. 34, no. 2, pp. 53–60, 2022.

[7] D. Xu, Y. Zheng, Y. Chu, Y. Wang, T. Shi, and X. Gu, "Generalized load collaborative and interactive dispatching strategy in smart communities based on reinforcement learning," *Power System and Clean Energy*, vol. 40, no. 2, pp. 84–94, 2024.

[8] X. Du, Q. Wu, and L. Xu, "Implementation mechanism and optimization path of resilience governance of digitally empowered communities under the concept of people-oriented city," *Journal of Xi'an Jiaotong University (Social Sciences Edition)*, vol. 44, no. 3, pp. 115–124, 2024.

[9] Y. Song, K. Shao, and Y. Wang, "Construction of smart community emergency service management system," *Internet of Things Technology*, vol. 12, no. 3, pp. 60–63, 2022.

[10] L. Yu and Y. Wang, "Exploration of implementation path to rural middle classisation under the context of Chinese rural revitalisation," *Economic Geography*, vol. 41, no. 2, pp. 167–173, 2021.

[11] J. Bricout, P. M. Baker, N. W. Moon, and B. Sharma, "Exploring the smart future of participation: Community, inclusivity, and people with disabilities," *International Journal of E-Planning Research*, vol. 10, no. 2, pp. 94-108, 2021.

Edelweiss Applied Science and Technology
ISSN: 2576-8484
Vol. 9, No. 6: 2305-2323, 2025
DOI: 10.55214/25768484.v9i6.8370

[12] R. Shen and M. Chen, "Development of the middle-income stratum under the new era," *Secretary*, vol. 41, no. 2, pp. 34–42, 2023.

[13] C. Zhang, "Rural community education practice for returning urban middle class: A case study of Mingguang Village," *Chinese Education: Research and Review*, vol. 25, no. 1, pp. 88–124, 2020.

[14] K.-F. Guo, H.-X. Jiang, T.-Q. Dai, and J.-P. Song, "A systematic review on smart communities in Western countries," *Human Geography*, vol. 39, no. 4, pp. 19–26, 2024.

[15] E. Blasch *et al.*, "Machine learning/artificial intelligence for sensor data fusion–opportunities and challenges," *IEEE Aerospace and Electronic Systems Magazine*, vol. 36, no. 7, pp. 80-93, 2021.

[16] J. D. Choi and M. Y. Kim, "A sensor fusion system with thermal infrared camera and LiDAR for autonomous vehicles and deep learning based object detection," *ICT Express*, vol. 9, no. 2, pp. 222-227, 2023.

[17] F. Altay and S. Velipasalar, "The use of thermal cameras for pedestrian detection," *IEEE Sensors Journal*, vol. 22, no. 12, pp. 11489-11498, 2022.

[18] D. Lee, M. Jung, W. Yang, and A. Kim, "Lidar odometry survey: recent advancements and remaining challenges," *Intelligent Service Robotics*, vol. 17, no. 2, pp. 95-118, 2024.

[19] Y. Chen, D. Sanz-Alonso, and R. Willett, "Autodifferentiable ensemble Kalman filters," *SIAM Journal on Mathematics of Data Science*, vol. 4, no. 2, pp. 801-833, 2022.

[20] M. Bai, Y. Huang, B. Chen, and Y. Zhang, "A novel robust Kalman filtering framework based on normal-skew mixture distribution," *IEEE Transactions on Systems, Man, and Cybernetics: Systems*, vol. 52, no. 11, pp. 6789-6805, 2021.

[21] A. Jabbari and J. B. Mohasefi, "A secure and LoRaWAN compatible user authentication protocol for critical applications in the IoT environment," *IEEE Transactions on Industrial Informatics*, vol. 18, no. 1, pp. 56-65, 2021.

[22] M. A. Ullah, K. Mikhaylov, and H. Alves, "Analysis and simulation of LoRaWAN LR-FHSS for direct-to-satellite scenario," *IEEE Wireless Communications Letters*, vol. 11, no. 3, pp. 548-552, 2021.

[23] P. Wlazlo *et al.*, "Man-in-the-middle attacks and defence in a power system cyber-physical testbed," *IET Cyber-Physical Systems: Theory & Applications*, vol. 6, no. 3, pp. 164-177, 2021.

[24] G. L. Jones and Q. Qin, "Markov chain Monte Carlo in practice," *Annual Review of Statistics and Its Application*, vol. 9, no. 1, pp. 557-578, 2022.

[25] D. Layden *et al.*, "Quantum-enhanced markov chain Monte Carlo," *Nature*, vol. 619, no. 7969, pp. 282-287, 2023.

[26] A. Onan, "Bidirectional convolutional recurrent neural network architecture with group-wise enhancement mechanism for text sentiment classification," *Journal of King Saud University-Computer and Information Sciences*, vol. 34, no. 5, pp. 2098-2117, 2022.

[27] A. Pramono, T. J. L. g. Tama, and T. Waluyo, "Analysis of three-phase current of 197 KVA power using the Kolmogorov-Smirnov normality test method," *Jurnal RESISTOR (Rekayasa Sistem Komputer)*, vol. 4, no. 2, pp. 213-216, 2021.

[28] Y. He and L. Xiao, "Structured pruning for deep convolutional neural networks: A survey," *IEEE Transactions on Pattern Analysis and Machine Intelligence*, vol. 46, no. 5, pp. 2900-2919, 2023.

[29] T. Mao, Z. Shi, and D.-X. Zhou, "Approximating functions with multi-features by deep convolutional neural networks," *Analysis and Applications*, vol. 21, no. 01, pp. 93-125, 2023.

[30] Q. Zhang *et al.*, "A method for measuring similarity of time series based on series decomposition and dynamic time warping," *Applied Intelligence*, vol. 53, no. 6, pp. 6448-6463, 2023.

[31] S. Bagui, D. Nandi, S. Bagui, and R. J. White, "Machine learning and deep learning for phishing email classification using one-hot encoding," *Journal of Computer Science*, vol. 17, no. 7, pp. 610-623, 2021. https://doi.org/10.3844/jcssp.2021.610.623

[32] C. P. Barlett *et al.*, "Cross-cultural similarities and differences in the theoretical predictors of cyberbullying perpetration: Results from a seven-country study," *Aggressive Behavior*, vol. 47, no. 1, pp. 111-119, 2021.

[33] M. R. Awal, R. K.-W. Lee, E. Tanwar, T. Garg, and T. Chakraborty, "Model-agnostic meta-learning for multilingual hate speech detection," *IEEE Transactions on Computational Social Systems*, vol. 11, no. 1, pp. 1086-1095, 2023.

[34] Y. Mo, L. Li, B. Huang, and X. Li, "Few-shot RUL estimation based on model-agnostic meta-learning," *Journal of Intelligent Manufacturing*, vol. 34, no. 5, pp. 2359-2372, 2023.

[35] J. Xu, C. Wang, and X. Jia, "A survey of blockchain consensus protocols," *ACM Computing Surveys*, vol. 55, no. 13s, pp. 1-35, 2023.

[36] Z. Ai and W. Cui, "A proof-of-transactions blockchain consensus protocol for large-scale IoT," *IEEE Internet of Things Journal*, vol. 9, no. 11, pp. 7931-7943, 2021.

Edelweiss Applied Science and Technology
ISSN: 2576-8484
Vol. 9, No. 6: 2305-2323, 2025
DOI: 10.55214/25768484.v9i6.8370

[37] R. Eyvazpour, M. Shoaran, and G. Karimian, "Hardware implementation of slam algorithms: a survey on implementation approaches and platforms," *Artificial Intelligence Review*, vol. 56, no. 7, pp. 6187-6239, 2023.

[38] X. Dong, L. Cheng, H. Peng, and T. Li, "FSD-SLAM: A fast semi-direct SLAM algorithm," *Complex & Intelligent Systems*, vol. 8, no. 3, pp. 1823–1834, 2022.

[39] B. Zaman, S. Z. Mahfooz, R. Mehmood, N. Khan, and T. Imran, "An adaptive EWMA control chart based on Hampel function to monitor the process location parameter," *Quality and Reliability Engineering International*, vol. 39, no. 4, pp. 1277-1298, 2023.

[40] M. A. Sarwar and M. Noor-ul-Amin, "Design of a new adaptive EWMA control chart," *Quality and Reliability Engineering International*, vol. 38, no. 7, pp. 3422-3436, 2022.

Edelweiss Applied Science and Technology
ISSN: 2576-8484
Vol. 9, No. 6: 2305-2323, 2025
DOI: 10.55214/25768484.v9i6.8370